Theoretical Study of the Potential Energy Surfaces of the Van Der Waals $H_2O-X_2{}^+$ (X = Cl or Br) Complexes

Tahra Ayed,[†,‡] **Ramón Hernández Lamoneda,**[*,†] **and Kenneth C. Janda**[‡]

Centro de Investigaciones Químicas, Universidad Autónoma del Estado de Morelos, Cuernavaca, Morelos 62210, Mexico, and Department of Chemistry, University of California at Irvine, Irvine, California 92697-2025

Received: October 8, 2007; In Final Form: November 1, 2007

An ab initio study of the interactions between H_2O and $Cl_2{}^+$ and H_2O and $Br_2{}^+$ has been performed. We present calculations using both the UMP2 level and the UCCSD(T) level of correlation with the aug-cc-pVTZ basis. The aug-cc-pVQZ basis was tested for selected geometries and was found to yield results similar to the smaller basis. For the $H_2O-Cl_2{}^+$ cation, a C_{2v} structure has been identified as the minimum, with D_e = 6500 cm^{-1} (78 kJ/mol). A low-lying excited state has D_e = 6000 cm^{-1} (72 kJ/mol). The adiabatic and vertical ionization energies of the complex are 10.7 and 11.0 eV, compared to the experimental adiabatic value, 11.5 eV, for free chlorine. For the $H_2O-Br_2{}^+$ cation, the calculations are more subtle due to second-order Jahn−Teller effects and result in a C_s structure at the minimum, with D_e = 6300 cm^{-1} (75 kJ/mol), yielding an adiabatic ionization energy of 9.9 eV compared to the corresponding experimental value, 10.5 eV, for free bromine. The relatively large binding energies give rise to strong normal mode couplings such that the halogen stretching mode becomes mixed with the water bending and other intermolecular modes, resulting in very large frequency shifts. Vertical ionization energies and ion vibrational frequencies also are reported and used to discuss possible experiments to obtain more precise data for each of the complexes.

I. Introduction

In 1976 it was discovered that the dimer of the interhalogen molecule ClF and the potential hydrogen bond donor molecule HF is stabilized by electron pair donation from the HF to the σ^* orbital on the Cl end of the ClF moiety rather than by the expected hydrogen bond to the fluorine atom.[1] Since then, there has been a rapidly expanding literature regarding electron pair donation to halogen molecules.[2,3] Legon and co-workers propose that the phenomenon is distinct enough to deserve its own name: halogen bonding.[4,5] Microwave spectra have been reported for both the H_2O-Cl_2 and the H_2O-Br_2 dimers. In each case, the O−X bond length is quite short, ∼2.85 Å, compared to the sum of the van der Waals radii, O, 1.52 Å; Cl, 1.75 Å; and Br, 1.85 Å. Recent calculations of the well depth for the neutral dimers using the CCSD(T) correlation method, an augmented quadruple-ζ basis set, and the counterpoise correction for basis set superposition error yielded 917 cm^{-1} (11 kJ/mol) for H_2O-Cl_2 and 1183 cm^{-1} (14 kJ/mol) for H_2O-Br_2.[6] These well depths are a significant fraction of the water dimer well depth, 1756 cm^{-1} (21 kJ/mol), and greater than the 8 kJ/mol well depth for the HCl dimer.[7] In addition, the H_2O-Cl_2 and the H_2O-Br_2 interactions were found to be very sensitive to the X−X distance. For instance, a modulation of the Br−Br bond by ±0.05 Å, approximately the classical amplitude for the ground vibrational state, modulates the O−X bond strength by over 100 cm^{-1}, 10% of the well depth. These results identify the water−halogen dimers as both interesting and complex with respect to their intermolecular forces.

There is also recent experimental data that illustrates that the interactions between water molecules and halogens are unusually complex and interesting. The peak of the Br_2 visible valence band excitation shifts 1700 cm^{-1} toward higher energy in going from the gas phase to aqueous solution. This blue shift has been attributed to the same neighbor donation of an oxygen atom lone electron pair from a water molecule to the Br_2 σ^* orbital that results in the relatively deep dimer well. Valence excitation of the bromine promotes an electron from the π^* orbital to the σ^* orbital, resulting in O−X repulsion in the excited state. In contrast, for bromine surrounded by water forming a nearly symmetric 6^45^{12} cage of a clathrate−hydrate crystal, the shift of the visible excitation band maximum from the gas phase is reduced to only 360 cm^{-1}. In this case the lone electron pairs of the water molecules are all involved in hydrogen bonding and thus less available to interact with the bromine molecule even though it is in close contact.

The unusual properties of neutral water−halogen dimers have inspired us to investigate the dimer cations. These species are interesting in their own right and also as a possible subject for multiphoton ionization (MPI) spectroscopy. The ionization potentials of H_2O, Cl_2, and Br_2 are, respectively, 12.62, 11.50, and 10.52 eV.[8,9] Thus the lowest ionization channel is expected to be removal of an electron from the halogen π^* orbital. In the isolated halogen, this results in a doubly degenerate electronic state. Interaction with the water splits this degeneracy, resulting in some interesting computational challenges. The $H_2O-Cl_2{}^+$ and the $H_2O-Br_2{}^+$ cations have different symmetries at their minima. Below, we explain the reasons for this difference. Although the neutral and cation dimers have somewhat different structures, they are similar enough that MPI spectroscopy should yield long-lived cation states that can be used to extract the rich vibrational structure that will provide significant insight into the intermolecular interactions. Also, MPI spectroscopy will be a useful technique for double resonance spectroscopy to obtain the neutral dimer vibrational spectrum.

* Author to whom correspondence should be addressed. E-mail: ramon@buzon.uaem.mx.
† Universidad Autónoma del Estado de Morelos.
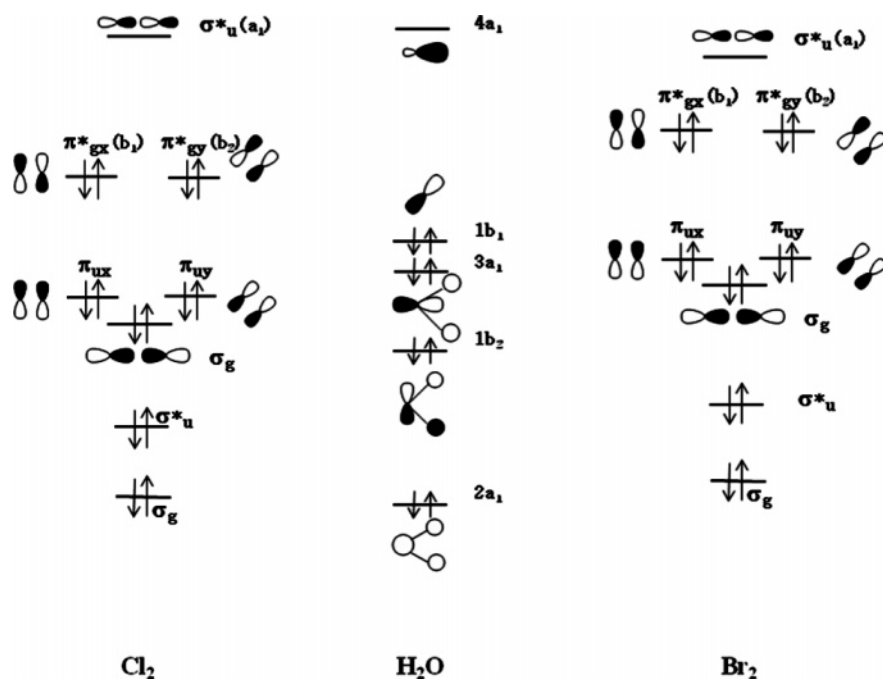‡ University of California at Irvine.

H2O−X2+ (X = Cl or Br) Complexes

J. Phys. Chem. A, Vol. 112, No. 4, 2008 **723**

Figure 1. Molecular orbital diagrams of Cl_2, H_2O, and Br_2.

II. Theoretical Details

The ground potential energy surfaces (PESs) of the cation $H_2O–X_2^+$ (X = Cl or Br) systems were studied using Møller–Plesset perturbation theory (MP2)[10,11] with the unrestricted formalism. The geometries of all of the stationary points are optimized using the aug-cc-pVTZ basis sets[12,13] and harmonic vibrational frequency analysis performed to identify minima and saddle points. In addition, we performed some intrinsic reaction coordinate (IRC) calculations to connect transition states and minima and also to locate other minima that were difficult to find. The relative stabilities of several optimized structures were evaluated also by single-point energy calculations at the open-shell coupled-cluster level taking into account the perturbative contributions of connected triple excitations UCCSD(T).[14] The zero-point energy (ZPE) correction also was calculated at the UMP2/aug-cc-pVTZ level. Both ZPE effects and higher-level correlation treatment are required to obtain reliable thermochemical information for these systems.
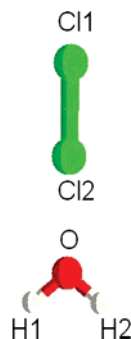
The effect of basis set saturation was tested at the UCCSD-(T) level by using both aug-cc-pVTZ and aug-cc-pVQZ.[15] The vertical transition energies have been calculated at this high level of theory. All of our calculations are full-electron and were performed with the Gaussian 03 program.[16]

III. Results and Discussion

A. Calculations for the Monomer Constituents. The starting point for our study was the calculation of the ionization potentials (IPs) for water and the two dihalogen molecules. In Table 1, we report adiabatic ionization energy values for H_2O, Cl_2, and Br_2 calculated at the UMP2 and UCCSD(T) levels of theory using the aug-cc-pVTZ basis set. (The small correction for ZPE is not included.) It is encouraging that theory values agree well with experiment and do not depend too strongly on the basis set or method used. It is interesting that the molecular orbital scheme illustrated in Figure 1 is sufficient for interpreting the ionization energies. The highest occupied molecular orbital (HOMO) of each dimer is the antibonding π^* type orbital of the X_2^+ fragment.

B. Results for $H_2O–Cl_2^+$. Due to the unpaired electron, the halogen cations have a degenerate ground state. Attaching a water molecule with a C_{2v} symmetry constraint (the symmetry axis is collinear with the dihalogen) leads to electronic states of B_1 and B_2 spatial symmetry because the unpaired electron occupies the π^*_{gx} orbital of b_1 symmetry or the π^*_{gy} orbital of b_2 symmetry, respectively. When decreasing the group of symmetry to C_s, the electronic states spatial symmetry will be A' and A''. The relevant structures are illustrated in Figures 2 and 3.

For $H_2O–Cl_2^+$, optimization at the UMP2 level of theory under the C_{2v} symmetry constraint reveals that both the B_1 and the B_2 electronic states correspond to local minima on their potential energy surfaces. The oxygen and the two chlorine atoms form the C_2 axis of symmetry. The C_{2v} structure is shown in Figure 2, the optimized molecular parameters are listed in Table 2, and the dissociation energies are given in Table 3. The B_1 electronic state, for which the unpaired electron occupies the orbital perpendicular to the plane containing all atoms, is more stable, by 614 cm^{-1}, than the B_2 electronic state in which the unpaired electron is in the plane of the molecule. This result is as expected because the b_1 orbital (π^*_{gx}) of the Cl_2^+ fragment is close in energy to the HOMO of water (one of the lone pairs) with the same symmetry. Therefore the two orbitals can interact strongly. For the B_2 electronic state, the unpaired electron occupies the b_2 orbital, and the interaction between this orbital and the water orbital of b_2 symmetry is small because the latter is a bonding orbital with lower energy. Mulliken population analysis shows that the chlorine atom near the oxygen becomes somewhat more positive, 0.59 and 0.58 in the B_1 and B_2 electronic states, respectively, compared to 0.50 for the isolated Cl_2^+. The Cl−Cl bond distance increases only slightly due to the interaction. In contrast, the calculated Cl−Cl stretching frequency is significantly higher (almost a factor of 2) for the complex than that for the free cation. Most likely the reason for the observed difference is due to the shortening of the O−X distance in the cation, 2.34 Å compared to 2.77 Å in the neutral compound, and the corresponding substantial increase in the binding energy of the complex that stiffens the Cl_2 stretching
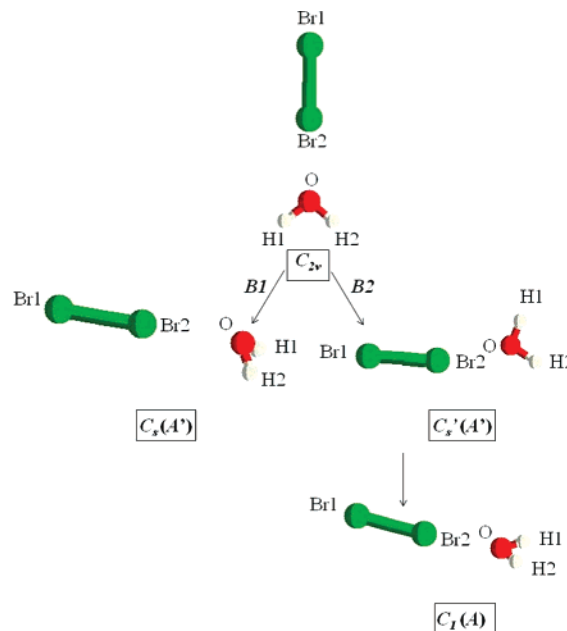
Figure 2. Geometry of the $H_2O-Cl_2^+$ complex at the global minimum.

Figure 3. Optimized structures of the $H_2O-Br_2^+$ complex calculated at the UMP2 level. Two electronic states have a C_{2v} structure that is a transition state. One relaxes to a C_s global minimum, and the second to another transition state with C_s symmetry. This final transition state relaxes to a secondary minimum with no symmetry (C_1) as shown.

motion within the complex. Furthermore looking at the corresponding normal mode we observe mixing of the chlorine stretching motion with the bending of the water molecule and the intermolecular stretch. Relatively small shifts are calculated for the normal modes of the water moiety in the complex. Note that the charge polarization and small shifts for water are also found in the case of the neutral dimer;[6] in that case the chlorine stretch showed a small shift from the monomer.

Both the B_1 and the B_2 electronic states exhibit one very low-frequency motion, 14 and 19 cm^{-1}, respectively. The low-frequency mode for the B_1 state has b_1 symmetry, and it exhibits bending of the water molecule out of the HOCl plane, whereas the low-frequency mode of the B_2 state has b_2 symmetry and exhibits bending of the water in the plane of the complex. An explanation of the low values and symmetries of these normal modes will be given later. Here we simply note that each state will exhibit wide-amplitude vibrational motion.

C. Results for $H_2O-Br_2^+$. The minima for the $H_2O-Br_2^+$ cation have C_s symmetry as illustrated in Figure 3. However, we show a preliminary analysis constraining the geometry to C_{2v} symmetry (using the UMP2/aug-cc-pVTZ level of theory) for comparison to the $H_2O-Cl_2^+$ results. The structural results are given in Table 4. The results at this level for the $H_2O-Br_2^+$ cation are similar to those for the $H_2O-Cl_2^+$ cation: a short O−Br bond, 2.5 Å, a high Br−Br stretching frequency, 825 cm^{-1}, with more modest changes in the other parameters relative to the free molecules. Frequency calculations for the B_1 and B_2 electronic states of $H_2O-Br_2^+$ yield small imaginary frequencies, 45i and 46i cm^{-1}, respectively, for the two modes that had small but real frequencies for $H_2O-Cl_2^+$. Thus these structures represent transition states between the real minima, indicating the need to relax the C_{2v} symmetry constraint.

To locate the minimum structure linked with this transition state we employed the IRC technique. This consists of following the imaginary frequency descent path from the transition state down to the minimum structure on the potential energy surface. Figure 4 shows the relative stability of each geometry calculated at UMP2 level when geometry constraints are relaxed as represented in Figure 3. The C_{2v}, B_1 transition state optimizes to a C_s structure with A′ electronic state symmetry, 76.4 cm^{-1} below the transition state. Thus this saddle point separates two equivalent minima. Correcting for ZPE raises the relative energy of the C_s structure back above that of the B_1 transition state (Figure 4). So, this level of theory predicts that the state will exhibit wide-amplitude motion, resulting in vibrational averaging to the more symmetric B_1 structure. Note that a significant fraction of the ZPE increase for the C_s minimum is due to the increased Br−Br stretching frequency, which is strongly coupled to the intermolecular stretch and bend and also the bending mode of the water moiety.

In the light of the UMP2 results, we decided to perform a single-point UCCSD(T)/aug-cc-PVTZ calculation using the UMP2/aug-cc-pVTZ geometries. At this higher level, the stability of the C_s structure relative to the B_1 transition state increases to 220.1 cm^{-1}. Adding ZPE corrections calculated at the UMP2 level to the relative electronic energy calculated at the UCCSD(T) level leaves the C_s structure more stable but only by 36.7 cm^{-1}. The flat surface for this bending coordinate indicates that it may be difficult to completely converge the calculation while including ZPE effects. Multiphoton ionization spectroscopy may be able to yield vibrational frequencies that will aid in a definitive assignment.

Further optimization of the C_{2v}, B_2 state of the $H_2O-Br_2^+$ cation yields even more complicated results. Following the normal mode of the imaginary frequency leads to a new saddle point structure having C_s symmetry rather than to the expected minimum. The symmetry of this electronic state is A′, and all the atoms of the complex lie in the plane of symmetry as shown in Figure 3. This structure will be denoted as C_s' and is 81 and 177 cm^{-1}, respectively, for UMP2/aug-cc-pVTZ and UCCSD-(T)/aug-cc-pVTZ below the B_2 state. As for the B_1 state, adding the UMP2 ZPE corrections to the UMP2 energy values reverses the relative stabilities of the B_2 and A′ transition states, while the ZPE correction to the UCCSD(T) results leaves the A′ state as the lower minimum by 27 cm^{-1}.

Further relaxation of the symmetry yields a C_1 minimum energy structure as illustrated in Figure 3. This structure is characterized by Br−Br and Br···O distances equal to 2.178 and 2.496 Å, which are similar to but distinguishable from those of the C_s minimum. Zero-point energy corrections leave this as the local minimum for both UMP2 and UCCSD(T). For UCCSD(T), the C_1 structure is 523 cm^{-1} below the C_s' saddle point and 551 cm^{-1} below the B_2 saddle point, including ZPE. Figure 4 summarizes the relative energies of the $H_2O-Br_2^+$ states for different levels of calculation. The C_s structure remains the global minimum but only by 24 cm^{-1} if ZPE effects are included. Table 4 gives the geometric parameters of both C_s and C_1 structures. We note that the main differences between

TABLE 1: Theoretical Values of the Ionization Energies (eV) Compared to the Experimental Values

	UMP2/aug-cc-pVTZ	UCCSD(T)/aug-cc-pVTZ	UCCSD(T)/aug-cc-pVQZ	expt.
H_2O	12.77	12.67	12.72	12.62^a
Cl_2	11.46	11.43	11.55	11.48^b
Br_2	10.60	10.44	10.57	10.52^b

^{a} Reference 8. ^{b} Reference 9.

TABLE 2: Main Geometric Parameters of the $H_2O-Cl_2^+$ Dimer Obtained from the UMP2/aug-cc-pVTZ Level of Calculations and Normal Mode Values of Water and Cl_2^+ Calculated at the Same Level

	monomer	$H_2O\cdots Cl_2^+$	
	(Cl_2^+, H_2O)	B_1 electronic state	B_2 electronic state
Cl1−Cl2	1.910	1.923	1.916
Cl2⋯O		2.343	2.421
Cl1−Cl2⋯O		180.0	180.0
H1−O−H2	104.1	105.8	105.3
$\nu_1 (a_1)^b$	1628	1641	1645
$\nu_2 (a_1)^b$	3822	3760	3777
$\nu_3 (b_2)^b$	3948	3874	3888
ν_{Cl-Cl}^b	639	1133	1081
$q(Cl1)^c$	0.50	0.40	0.42
$q(Cl2)^c$	0.50	0.59	0.58

^{a} Bond lengths in are Å, and bond angles in degrees. ^{b} Wavenumbers are in cm^{-1}. ^{c} Atomic charge calculated at the UMP2 level from Mulliken population analysis.

these two minima are the value of the Br−Br−O angle, which is equal to 165.3° in the former and 175.7° in the latter, and the Br−Br−O−H dihedral angles.

D. Comparison of $H_2O-Cl_2^+$ and $H_2O-Br_2^+$. As illustrated above, symmetry breaking for $H_2O-Br_2^+$ results in significant differences from the potential energy surface of the $H_2O-Cl_2^+$ cation. The stabilities of the C_{2v} structures for both chlorine and bromine complexes can be rationalized by invoking the well-known second-order Jahn−Teller (SOJT) effects.[18] Looking at the MO diagram of Figure 1, we can predict that a low-lying excited state is obtained by promoting the unpaired electron from the π^*_{gx} or π^*_{gy} orbitals to a σ^*_u orbital. Within the C_{2v} symmetry, the corresponding electronic state symmetries are B_1, B_2, and A_1. Application of the SOJT suggests that for the $^2B_1$ electronic state there will be an important contribution to lower the vibrational frequency of modes with b_1 symmetry; analogously for the $^2B_2$ electronic state low-frequency modes of b_2 symmetry are expected. Indeed in the case of chlorine the lowest frequencies belong to these symmetries for the corresponding, B_1 and B_2, electronic states: 14 and 19 cm^{-1}. In the case of bromine, the C_{2v} structures are unstable with respect to SOJT effects, leading to transition states with imaginary frequencies of expected symmetries and values of 45i and 46i cm^{-1}. The difference in chlorine and bromine is consistent with the fact that the energy difference between π^* and σ^* is smaller in the latter. Still the values for all of these frequencies are small enough to establish a challenge for accurate predictions using ab initio quantum chemistry. The second saddle point found for the bromine complex in C_s symmetry (the C_s' structure in Figure 3) also can be rationalized using SOJT effects, though the argument involves a different excited electronic state: In this case the promotion is out of the doubly occupied π^* orbital because this will lead to an excited state of the complex of a'' symmetry consistent with an imaginary frequency for a normal mode of that same symmetry as observed in the calculations.

Finally, we note that the large increase in the dihalogen stretching frequency upon complexation has no simple correlation with a change in dihalogen bond length. In the case of chlorine, the bond length increases, perhaps contrary to chemical

intuition. The case of bromine is more complicated due to the variety of structures found. For the C_{2v} structures, analogous to chlorine, the bond length decreases noticeably (0.02−0.03 Å), but in the case of all other structures the change in bond length is less marked, and in particular for the global minimum it is negligible.

E. Vertical Ionization Calculations. The highest intensity for nonresonant MPI spectroscopy will be in the region of vertical ionization. Therefore it is useful to both calculate the vertical ionization energies and examine how high the levels of the ions are over the adiabatic minima. Both the H_2O-Cl_2 and the H_2O-Br_2 neutral dimers have C_s symmetry similar to that shown in Figure 3 with a small barrier at the C_{2v} structure. For the purpose of this study, we calculated the vertical ionization energy from the global minimum to each of the two cation states. Table 3 lists the results using both the UMP2 and the UCCSD(T) levels of theory with the aug-cc-pVTZ basis. The UMP2 energy values corresponding to the $^1A'-^2A'$ and $^1A'-^2A''$ vertical transitions are equal to 10.99 and 11.01 eV for H_2O-Cl_2 and to 10.12 and 10.20 eV for H_2O-Br_2. Thus the state splittings for the cations are relatively small at the neutral geometry. These results were confirmed by the UCCSD-(T) calculations.

Figure 5 shows the potential energy curves as a function of the O−Br distance for both the neutral H_2O-Br_2 and the cation complex calculated with UCCSD(T)/aug-cc-pVTZ. The symmetry and angles are fixed at the corresponding values for each minimum geometry. Although the equilibrium Br−O bond length for the neutral compound, 2.8 Å, is significantly longer than that for the cation complex, 2.5 Å, the much deeper well for the cation means that vertical ionization leaves the cation well below its dissociation limit. As discussed above, we expect there to be strong bend stretch coupling for the cation, so there should be strong progressions in several modes, probably spreading to the adiabatic minimum energy. This prediction has two important implications for the experiment. First, it should be possible to excite to near the ground state of the cation, yielding a long-lived state that will allow mass selection. This will allow MPI to be used as a detection technique to obtain mass-selected infrared spectroscopy of the neutral dimer. Second, the extensive vibrational structure expected for the cation could yield an accurate determination of its PES. Given the complexity of the systems, analysis of the vibrational structure will require careful comparisons between the experiment and the theory.

F. Possible Calculations for Larger Clusters. Eventually, we hope to extend these studies to larger clusters with hopes of helping to interpret the condensed phase experiments discussed in the Introduction. In that regard, the relative insensitivity of the well depths and ionization energies to the basis set and level of theory is encouraging. It appears that UMP2/aug-cc-pVTZ calculations provide a reliable option to investigate the addition of more water molecules to both the neutral halogens and their cations.
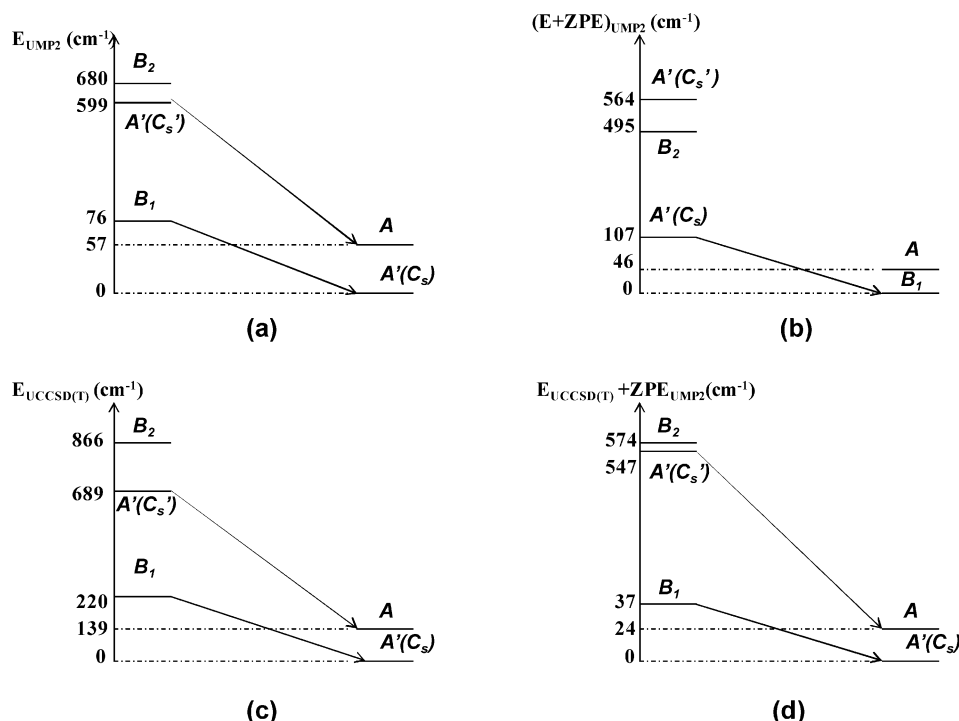
Figure 4. (a) Relative energies of each $H_2O-Br_2^+$ structure with reference to the global minimum calculated at UMP2 level without the ZPE corrections; (b) the corrected UMP2 relative energy; (c) the UCCSD(T) single-point energy; and (d) the UCCSD(T) single-point energy corrected with the UMP2 ZPE corrections.

TABLE 3: Dissociation Energy and Vertical Transition Values of Both Chlorine and Bromine Complexes Calculated at the UMP2 and UCCSD(T) Levels of Theory with the aug-cc-pVTZ Basis Set

	UMP2 level[a]		UCCSD(T) level[b]	
	$H_2O-Cl_2^+$	$H_2O-Br_2^+$	$H_2O-Cl_2^+$	$H_2O-Br_2^+$
D_e	7113 (0.88) (B_1)	6971 (0.86)	6515 (0.81) (B_1)	6088(0.76)
	6498 (0.81) (B_2)	(C_s, A')	5989 (0.74) (B_2)	(C_s, A')
			6770 (0.84) (B_1)[b]	6322(0.78)
			6169 (0.76) (B_2)[b]	(C_s, A')[b]
		Vertical Transition		
$^1A'-^2A'$	88 657 (10.99)	81 583 (10.12)	88 963 (11.03)	81 946(10.16)
$^1A'-^2A''$	88 799 (11.01)	82 269 (10.20)	89 124 (11.05)	82 591(10.24)

[a] Values are in cm^{-1}; the values between parentheses are in eV. [b] Values are calculated with the aug-cc-pVQZ basis set.

TABLE 4: Selected Bond Distances (Å), Angles (deg), and Frequencies (cm^{-1}) for the Transition States and Minima Structures of the $H_2O-Br_2^+$ Dimer Optimized at the UMP2 Level

|		C_{2v}(TS)		C_s(Br1−Br2−O−H1≠0)	C_s'	C_1
electronic state	Br_2^+	B_1	B_2	A'	A'	A
Br1−Br2	2.199	2.176	2.169	2.198	2.195	2.178
Br2···O		2.497	2.540	2.465	2.542	2.496
Br1−Br2···O		180.0	180.0	165.	163.4	175.7
Br2−O−H1(2)		127.4	127.5	127.2	127.9	127.7 (127.2)
Br1−Br2−O−H1(2)		180.0	180.0	88.0	0.0	−81.1(99.6)
ν_1 (a_1)[b]		1641	1640	1675(a')	1674(a')	1676(a)
ν_2 (a_1)[b]		3760	3778	3773(a')	3778(a')	3777(a)
ν_3 (b_2)[b]		3871	3888	3874(a'')	3883(a')	3879(a)
ν_{Br-Br}[b]	374	823	743	1002	975	801
q(Br1)[c]	0.50	0.40	0.42	0.38	0.39	0.39
q(Br2)[c]	0.50	0.57	0.55	0.59	0.59	0.58

[a] Bond lengths are in Å, and bond angles in degrees. [b] Wavenumbers are in cm^{-1}. [c] Atomic charge calculated at the UMP2 level from Mulliken population analysis.

IV. Summary and Conclusions

In the present study, we performed ab initio calculations of the PESs of the dihalogen−water cation complexes (chlorine and bromine). The UMP2/aug-cc-pVTZ level of theory was employed to optimize the geometries of all stationary points. The C_{2v} structures corresponding to the B_1 and B_2 electronic states were identified as minima for $H_2O\cdots Cl_2^+$, whereas they are first-order saddle points for the bromine complex. For the latter, a C_s symmetry structure, analogous to the neutral compound, has been identified as the global minimum and correlating with the B_1 transition state. Following the imaginary frequency coordinate characterizing the B_2 electronic state, we

H$_2$O−X$_2^+$ (X = Cl or Br) Complexes

J. Phys. Chem. A, Vol. 112, No. 4, 2008 **727**
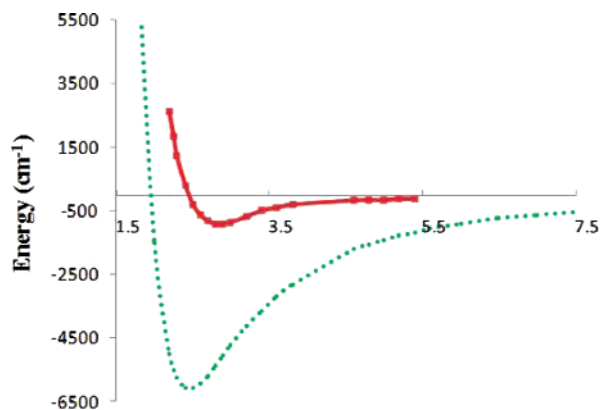
Figure 5. Potential energy curves of the bromine complexes (cation complex in dashed line and neutral complex in solid line) calculated at the UCCSD(T)/aug-cc-pVTZ level of theory. The *x*-axis gives the center of mass separation, Å, between the Br$_2$ and the H$_2$O at the geometry of each dimer minimum.

had found a second saddle point (C_s'). Upon further optimization one reaches a local minimum without symmetry and that lies only 24 cm^{-1} above the global minimum at the highest level of theory.

The main features of the PES were rationalized invoking the SOJT effect. Due to the small energy barriers and variety of isomers, it was deemed necessary to perform higher-level calculations that consisted of single-point UCCSD(T)/aug-cc-pVTZ with the UMP2/aug-cc-pVTZ geometries as references. The electronic energy ordering for each bromine structure remains the same as that for the UMP2 calculations. Finally, ZPE corrections calculated at the UMP2/aug-cc-pVTZ level were added to the UCCSD(T) values to obtain the most reliable estimates for the stabilities of the different structures.

The vertical transition energies were calculated for both chlorine and bromine systems. We find that the A′ and the A″ electronic states corresponding to the same cation complex are very close in energy and that the IP of the bromine complex is smaller than the IP of the chlorine complex. The effect of the basis sets has been tested, and the theoretical results show a small difference between the dissociation energy values calculated at the UCCSD(T) level with the aug-cc-pVTZ basis and the ones calculated at the same level and with the aug-cc-pVQZ basis. The bromine PESs are quite flat. This, along with the near degeneracy of the electronic states, makes a detailed characterization of the surfaces challenging. Also, wide-amplitude motion and ZPE effects may yield average structures somewhat different from the minima. Thus, although the present results will be valuable for an experimental search of these

cations, a detailed assignment of the spectra will still be complex. Finally, we note the very large shifts in the halogen stretching mode upon complex formation due to strong mixing with the bending mode of water and intermolecular modes.

References and Notes

(1) Nowick, S. E.; Janda, K. C.; Klemperer, W. *J. Chem. Phys.* **1976**, *65*, 5115.

(2) Legon, A. C.; Thumwood, J. M. A.; Waclawik, E. R. *Chem.−Eur. J.* **2002**, *8*, 940.

(3) Davey, J. B.; Legon, A. C.; Thumwood, J. M. A. *J. Chem. Phys.* **2001**, *114*, 61.

(4) Nguyen, H. L.; Horton, P. N.; Hursthouse, M. B.; Legon, A. C.; Bruce, D. W. *J. Am. Chem. Soc.* **2004**, *126*, 16.

(5) Legon, A. C. *Angew. Chem., Int. Ed.* **1999**, *38*, 2686.

(6) Hernández-Lamoneda, R.; Uc Rosas, V. H.; Bernal-Uruchurtu, M. I.; Halberstadt, N.; Janda, K. C. *J. Phys. Chem. A*, in press.

(7) Bunker, P. R.; Epa, V. C.; Jensen, P.; Karpfen, A. *J. Mol. Spectrosc.* **1991**, *146*, 200.

(8) Potts, A. W.; Prince, W. C. *Proc. R. Soc. London., Ser. A.* **1972**, *326*, 181.

(9) Yencha, A. J.; Hopkirk, A.; Hiraya, A.; Donovan, R. J.; Goode, J. G.; Maier, R. R. J.; King, G. C.; Kvaran, A. *J. Phys. Chem.* **1995**, *99*, 7231.

(10) Head-Gordon, M.; Pople, J. A.; Frisch, M. J. *Chem. Phys. Lett.* **1988**, *153*, 503.

(11) Frisch, M. J.; Head-Gordon, M.; Pople, J. A. *Chem. Phys. Lett.* **1990**, *166*, 275.

(12) Dunning, T. H., Jr. *J. Chem. Phys.* **1989**, *90*, 1007.

(13) Kendall, R. A.; Dunning, T. H., Jr.; Harrison, R. J. *J. Chem. Phys.* **1992**, *96*, 6796.

(14) Watts, J. D.; Gauss, J.; Bartlett, R. J. *J. Chem. Phys.* **1993**, *98*, 8718.

(15) Woon, D. E, Dunning, T. H., Jr. *J. Chem. Phys.* **1993**, *98*, 1358.

(16) Frisch, M. J.; Trucks, G. W.; Schlegel, H. B.; Scuseria, G. E.; Robb, M. A.; Cheeseman, J. R.; Zakrzewski, V. G.; Montgomery, J. A., Jr.; Stratmann, R. E.; Burant, J. C.; Dapprich, S.; Millam, J. M.; Daniels, A. D.; Kudin, K. N.; Strain, M. C.; Farkas, O.; Tomasi, J.; Barone, V.; Cossi, M.; Cammi, R.; Mennucci, B.; Pomelli, C.; Adamo, C.; Clifford, S.; Ochterski, J.; Petersson, G. A.; Ayala, P. Y.; Cui, Q.; Morokuma, K.; Salvador, P.; Dannenberg, J. J.; Malick, D. K.; Rabuck, A. D.; Raghavachari, K.; Foresman, J. B.; Cioslowski, J.; Ortiz, J. V.; Baboul, A. G.; Stefanov, B. B.; Liu, G.; Liashenko, A.; Piskorz, P.; Komaromi, I.; Gomperts, R.; Martin, R. L.; Fox, D. J.; Keith, T.; Al-Laham, M. A.; Peng, C. Y.; Nanayakkara, A.; Challacombe, M.; Gill, P. M. W.; Johnson, B.; Chen, W.; Wong, M. W.; Andres, J. L.; Gonzalez, C.; Head-Gordon, M.; Replogle, E. S.; Pople, J. A.*Gaussian 03*, revision C.02; Gaussian, Inc.; Wallingford CT, 2004.

(17) Ramondo, F.; Sodeau, J. R.; Roddis, T. B.; Williams, N. A. *Phys. Chem. Chem. Phys.* **2000**, *2*, 2309.

(18) Simons, J. *Energetic Principles of Chemical Reactions*; Jones and Bartlett Publishers: Boston, 1983.